A Reciprocating Delivery Device-Based Endovascular Intervention Robot With Multimanipulators Collaboration

Sheng Cao, *Graduate Student Member, IEEE*, Shuxiang Guo, *Fellow, IEEE*, Jian Guo, Jian Wang, Yongxin Zhang, Yongwei Zhang, Pengfei Yang, and Jianmin Liu

***Abstract*— The cardio-cerebrovascular disease is a significant disease that can directly threaten life and health. Vascular intervention surgery is currently the mainstream treatment method. This kind of surgery requires doctors to be exposed to radiation for a long, with extensive body damage. In response, domestic and foreign researchers began to develop endovascular intervention surgery robots. Although the robot has specific additional capabilities, it is still in the research and development stage. It must continuously improve performance, reliability, and functionality before it can be used in interventional surgery. Therefore, to further reduce doctors' learning and training costs, optimize the operation steps in surgery, and improve delivery accuracy, we developed a reciprocating delivery device-based endovascular intervention robot with multimanipulators collaboration. The third-party type test confirmed that the robot's feasibility and overall performance meet the surgery's needs (average linear accuracy is less than 0.1 mm). In vivo experiments have demonstrated the efficacy, safety, and reduction of radiation exposure to doctors (nearly 98.68%).**

***Index Terms*— Collaboration, control system, endovascular intervention robot, multimanipulators, reciprocating delivery device.**

I. Introduction

ON NOVEMBER 16, 2022, the global population exceeded 8 billion. However, the birth rate is constantly decreasing, and the challenge of aging has become a world problem. On the one hand, there is a shortage of labor. On the other hand, the diagnosis and treatment of cardiovascular diseases (CVDs) in a large aging population need to be met, according to the statistics released by the American Heart Association (AHA) in 2022. CVD claims more lives each year in USA than all forms of cancer and chronic lower respiratory disease (CLRD) combined. Among non-Hispanic (NH) Asian adults 20 years of age and older between 2015 and 2018, 52.0% of males and 42.5% of females had CVD. Cather-guided interventional surgery has many advantages as the primary medical method to solve vascular stenosis and embolism [1], [2].

It is a minimally invasive surgery, which causes minor trauma, improves symptoms quickly, recovers wounds rapidly, does not affect the social activities, and can repeatedly perform surgery under the condition of need, with low postoperative adverse reactions. Second, it is a precise targeted treatment method, which, in combination with digital subtraction angiography (DSA), makes the operation process more intuitive and provides more direct information feedback to doctors. However, it still requires doctors to have considerable clinical experience and to wear heavy lead clothing during the whole operation process to reduce the impact of radiation, which not only increases the training cost of vascular interventional surgeons but also affects the health of doctors [3], [4].

Therefore, to solve the above problems, many institutions began to study endovascular intervention robots, hoping to reduce the radiation damage to doctors, balance medical resources, reduce the training costs of interventional doctors, and use artificial intelligence, image processing, and other technologies to assist doctors in achieving accurate positioning and improving the operation safety [5], [6], [7], [8], [9], [10], [11], [12]. Among them, the Sensei X2 robot system developed by Hansen Medical in USA can realize active bending delivery using a specially customized catheter through the master–slave operation. Still, it is not compatible with commercial catheters of other specifications and brands on the market. The R-One robot-assisted percutaneous coronary intervention (PCI) system developed by the French Robopath company comprises a radiation protection console and an intervention robot. The catheter and guidewire are delivered from the end robot through the rocker operation. It adopts an open architecture and is compatible with the mainstream intervention devices on the market. The CorPath GRX system Siemens developed includes the slave operation controller and

Manuscript received 13 October 2023; accepted 27 November 2023. Date of publication 14 December 2023; date of current version 29 December 2023. This work was supported in part by the National Natural Science Foundation of China under Grant 61703305 and in part by the National High-Tech Research and Development Program (863 Program) of China under Grant 2015AA043202. The Associate Editor coordinating the review process was Dr. Damodar Reddy Edla. *(Corresponding author: Shuxiang Guo.)*

Sheng Cao is with the School of Life Science, Beijing Institute of Technology, Beijing 100081, China.

Shuxiang Guo is with the Department of Electronic and Electrical Engineering, Southern University of Science and Technology, Shenzhen 518055, China, and also with the School of Life Science and the Key Laboratory of Convergence Medical Engineering System and Healthcare Technology, Ministry of Industry and Information Technology, Beijing Institute of Technology, Beijing 100081, China (e-mail: guo.shuxiang@sustech.edu.cn).

Jian Guo and Jian Wang are with Shenzhen Institute of Advanced Biomedical Robot Company Limited, Shenzhen 518000, China.

Yongxin Zhang, Yongwei Zhang, Pengfei Yang, and Jianmin Liu are with the Neurovascular Center, Changhai Hospital, Naval Medical University, Shanghai 200433, China.

Digital Object Identifier 10.1109/TIM.2023.3342853

1557-9662 © 2023 IEEE. Personal use is permitted, but republication/redistribution requires IEEE permission.
See https://www.ieee.org/publications/rights/index.html for more information.

Authorized licensed use limited to: Shenzhen Technology University. Downloaded on January 02,2024 at 13:21:42 UTC from IEEE Xplore. Restrictions apply.

the master operation console. The slave operation controller comprises a mechanical arm and an intubation mechanism, with two degrees of freedom of linear motion and rotation. The intubation mechanism extrudes the catheter through a pair of controllable friction wheels. The central console mainly includes a medical image display screen and operating handle. The system can select interventional devices according to doctors' operation needs and patients' conditions and is equipped with the techIQ-Smart Procedural Automation function to assist doctors in achieving intelligent operations. Liberty is a disposable interventional surgery robot developed by Microbot Medical in the USA. It has a compact design and remote operation function. The control system can be tied to the patient's thigh. Doctors can push and operate the guidewire, catheter, and other instruments through the handheld remote controller. The one-time design reduces the maintenance cost and the hospital's fixed asset investment. The system is compatible with most commercial guidewires and catheters. The Massachusetts Institute of Technology (MIT) team developed a magnetically controlled flexible robot in 2022, which contains the motion of the flexible robot in the blood vessel through the magnetically controlled platform composed of the mechanical arm and the magnet. When the robot reaches the designated position, the doctor can send the catheter into and withdraw the robot, thus building the endovascular treatment pathway [13], [14], [15], [16], [17], [18].

The above studies are based on the master–slave split architecture design, which reduces the radiation damage to doctors through remote operation. However, there are still areas that need to be improved in these systems.

1) The operation mode of the master–slave is mainly based on the rocker. Doctors' clinical experience in surgery of hand movement needs to be changed, which will increase the learning cost and require doctors to make more adaptations and training.
2) Traditional roller-based delivery device often suffers from the challenges: excessive clamping force, leading to coating material damage and radial deformation, or inadequate clamping force resulting in simultaneous rolling and sliding, which affects delivery accuracy.

We have designed a reciprocating delivery device-based endovascular intervention robot with multimanipulators collaboration. The control system of the robot is divided into two parts, the master controller and the slave actuator.

The master controller uses a double-push rod design to simulate the holding mode of the catheter or guidewire and simulates the forward and backward through axial movement; radial motion simulates the rotation of the guidewire and catheter, thus establishing a human–robot interaction mode that preserves the doctor's operating habits. The slave actuator manipulator adopts the reciprocating delivery design.

The synchronization of the doctor's hand to the robot's action is realized through the master–slave cooperative strategy and control algorithm. The manipulator uses the two-plane passive clamping catheter and guidewire, which can be compatible with most of the interventional devices on the market. The mutual movement between the planes generates the torque, and the twisting function is realized. Relying on theoretical mechanics analysis, the traditional roller-based delivery device often suffers from challenges: excessive clamping force, leading to coating material damage and radial deformation, or inadequate clamping force resulting in simultaneous rolling and sliding, which affects delivery accuracy. The reciprocating delivery device in our article only requires the clamping to hold the interventional instrument axially. The main contributions of this article are as follows.

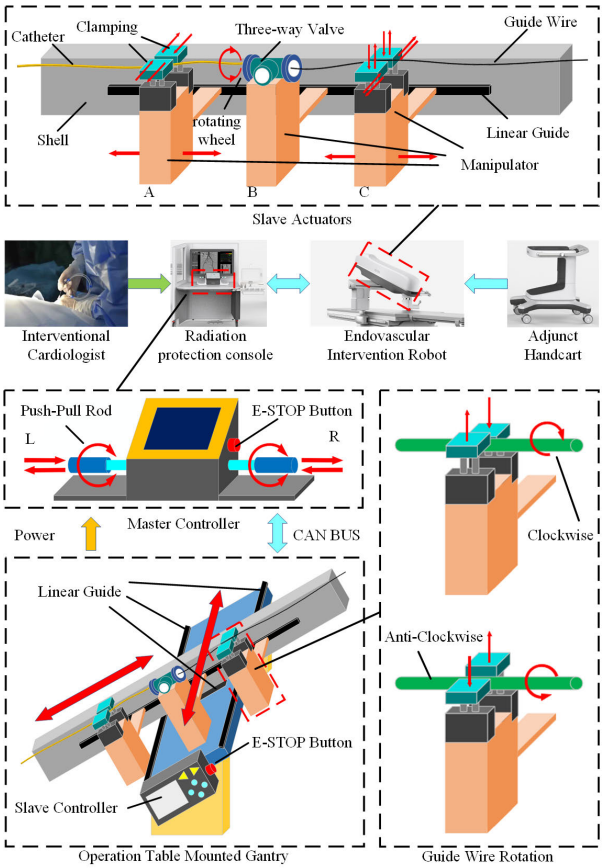

Fig. 1. Function diagram of endovascular intervention robot.

1) A novel method for the cooperative control of catheters and guidewire is proposed in this article. The double-push rod of the master controller emulates the operations of the catheter and guidewire, preserving the clinical experience for doctors.
2) The robot achieves tracking of hand movements with an average delivery accuracy of less than 0.1 mm. Doctors have successfully conducted 12 in vivo experiments, providing empirical evidence of the feasibility, safety, and efficacy of the robot.

This section clarifies the background significance and problems that need further improvement. Section II will introduce the overall framework of the endovascular intervention robot we developed.

II. Overview of Endovascular Intervention Robot

The endovascular intervention robot we developed comprises the radiation protection console, endovascular intervention robot, and adjunct handcart shown in Fig. 1.

Authorized licensed use limited to: Shenzhen Technology University. Downloaded on January 02,2024 at 13:21:42 UTC from IEEE Xplore. Restrictions apply.

The first part introduces the radiation protection console, which includes the master controller, radiation shielding glass, medical information display screen, and accessory slide rail. The primary function of the accessory slide rail is to fix the controller of other medical devices so that doctors can quickly switch between different devices.

For example, while operating the catheter and guidewire, they can also use the DSA device for imaging. At the same time, the doctor can directly see the patient's DSA image and physiological signal on the medical information display screen of the radiation protection console.

The display screen adopts hardware split screen processing, providing three independent display areas, which can be connected to different imaging devices, providing intuitive visual information.

For the first problem to be improved, the master controller is based on the operating habits of doctors. Its main components include a push–pull rod, stepping motor, linear slide, linear magnetic encoder, rotary grating encoder, contact induction switch, photoelectric switch, touch screen, emergency stop button (E-Stop button), and embedded computing device. The push–pull rod is fixed on the slide rail and contains a contact induction switch inside. The sensitivity of the contact induction switch can be adjusted by setting circuit parameters to improve the operation sensitivity of the doctor when wearing gloves. When the push–pull rod moves along the axial direction, the linear magnetic encoder can collect the displacement data of the rod. When the push–pull rod reaches the position and is released, the stepping motor can drive the rod to realize automatic homing and wait for the next operation. The rotary grating encoder will collect the rotation angle when the doctor rotates the push–pull rod. Because no round-trip movement is involved, the rotation does not need automatic homing. This structural design allows doctors to still control the catheter with the left hand and the guidewire with the right hand according to the previous operating habits. When the finger pinches the push–pull rod, the contact induction switch will be activated, and the slave actuator will hold the corresponding interventional device. The catheter will move forward or backward when the left push–pull rod is delivered or withdrawn. When the right push–pull rod is delivered or withdrawn, the guidewire will move forward or backward, while the axial movement is in progress, it will not affect the rotation of the rod, and there is no conflict between them. The primary function of the touch screen between the push–pull rod is to guide the doctor to initialize the operation, replace the interventional instrument, suspend the operation, and provide delivery mode switching and touch operation. Various alarm information prompts help the doctor achieve more accurate control and security. In an emergency, the E-Stop button next to it is connected in series with the main circuit of the power supply, which can directly cut off the motor power supply of the slave actuator to deal with the impact of emergencies during the operation.

The endovascular intervention robot includes the slave actuator and the operation table-mounted gantry. The slave actuator adopts the reciprocating delivery design and cooperates with the operation mode of the master controller. This corresponds to the doctor's hand operation, which tracks the hand's speed and position and restores the operation method. It helps the doctor realize some complex action mapping based on the previous operation experience. The slave actuator consists of a front-end fixed frame, three manipulators, a linear guide rail, linear encoders, screw stepper motors, photoelectric switches, and hall switches. The front-end fixing frame is fixed with the body of the slave actuator, which supports the catheter and connects the blood vessel sheath to ensure that the manipulator does not twist during the reciprocating delivery process.

The clamping functions of manipulators A and C are the same, and they are achieved by controlling the electromagnet. However, manipulator C will use the plane relative motion to generate torque, thus rotating the guidewire. Manipulator A does not have the function of rotating the catheter and needs to rely on manipulator B to realize the rotation of the catheter. Robot B differs from A and C. Its primary function is to fix the three-way valve, connect the high-pressure injection, the end of the catheter, and the front of the guidewire, and rotate the end. The operating table-mounted gantry is responsible for supporting the slave actuator and fixing it on the operating table. Through the slave controller, the slave actuator can be controlled to move in the plane along the linear guide rail and adjust the appropriate intervention position. In addition to changing the slave actuator, the slave controller is also equipped with a touch screen to realize the installation and replacement of instruments. We designed a disposable quick-release sterile box and a double-plane clamping mechanism. The sterile box can be easily placed on the manipulator.

The Hall switch can sense whether the sterile box is installed in place shown in Fig. 2. Then, the doctor can directly place the catheter or guidewire on the sterile box without any interposing action. When the interventional device needs to be replaced during the operation, the operation can be suspended by the slave controller. The catheter and guidewire can be replaced quickly to save operation time, improve the efficiency of doctors, and reduce the errors caused by complex steps. The double-plane clamping mechanism simulates the doctor's finger clamping mode. It can directly clamp the catheter and guidewire, which is highly compatible with them on the market. There are two main functions of the adjunct handcart. The first is to transport and store the robot. A single person can move easily and save space in the operation room. The second is to fix the whole robot on the slide rail of the operating table. By lifting the operating table and aligning the slide rail of the handcart, the entire endovascular intervention robot can be directly transferred from the adjunct handcart to the operating table along the slide rail. This section introduces the composition and function of the whole system of the endovascular intervention robot. The connection relationship between the components can be seen. Our solutions are given for the problems raised in Section I. Section III will introduce the intravascular intervention robot's module design and control system.

Authorized licensed use limited to: Shenzhen Technology University. Downloaded on January 02,2024 at 13:21:42 UTC from IEEE Xplore. Restrictions apply.

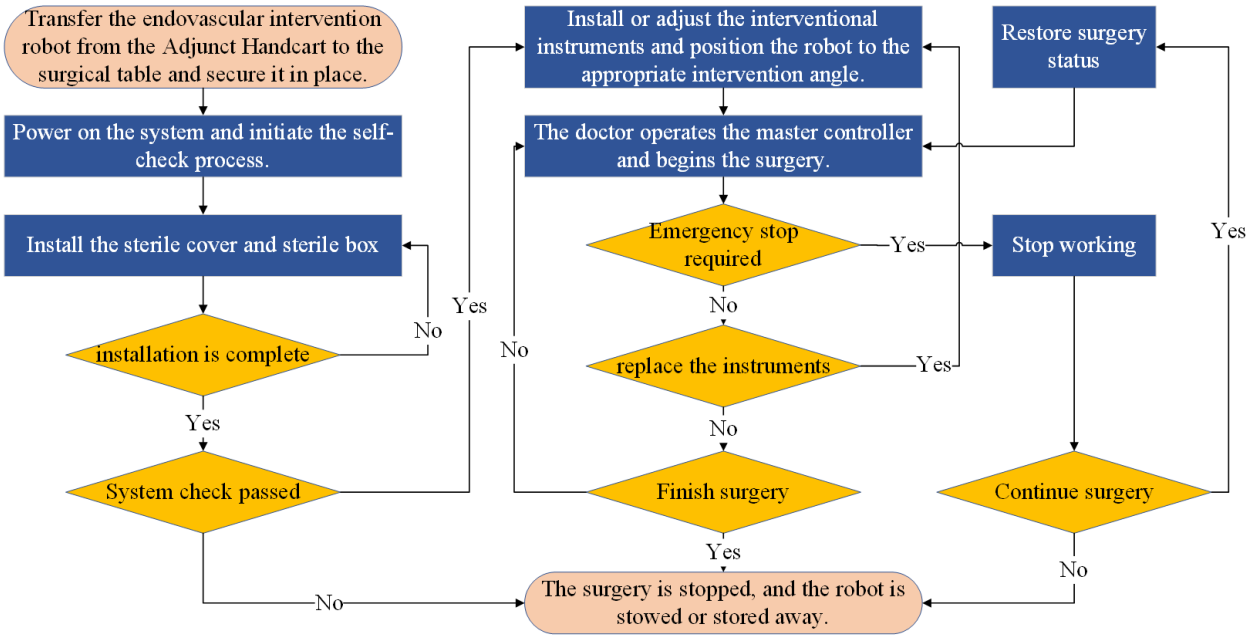

Fig. 2. Operation process diagram of robot for endovascular interventional procedures.

III. Design and Control of Multimanipulators

A. Manipulator Design

The slave robot has three manipulators to achieve different functions, as shown in Fig. 3: catheter clamping manipulator A, catheter rotating manipulator B, and guidewire clamping rotating manipulator C. Each manipulator includes a guide rail stepper motor, a linear encoder reading head, a manipulator control board, a motor drive board, hall switches, and photoelectric switches. To achieve the delivery function, the guide rail stepper motor can drive the entire manipulator forward and backward along the axial direction. At the same time, the linear encoder collects the pulse of the magnetic ruler and records the displacement data. The manipulator control board uses STM32 as the core microcontroller unit (MCU), receives the command information and various sensor data from the slave control board, and sends the generator movement command to the motor drive board or directly controls the electromagnet. The primary function of the hall switch is to identify whether the disposable sterile box is installed in place, and the operation will not start until the buckle part is firmly seated. The photoelectric switch is placed on each manipulator to limit the range of movement and prevent collision between the manipulators.

The robot facilitates the simultaneous movement of catheter and guidewire, while the manipulator enables both axial movement and radial rotation to occur simultaneously. The doctor can simultaneously control the motion status, including position and speed, such as varying the speed while advancing during rotation within a small distance range, which facilitates easier entry into vascular bifurcations.

The delivery and rotation function of the catheter is mainly completed by manipulators A and B. As shown in Fig. 4, manipulator A is only responsible for clamping and delivery, and the electromagnet realizes its clamping function. When the

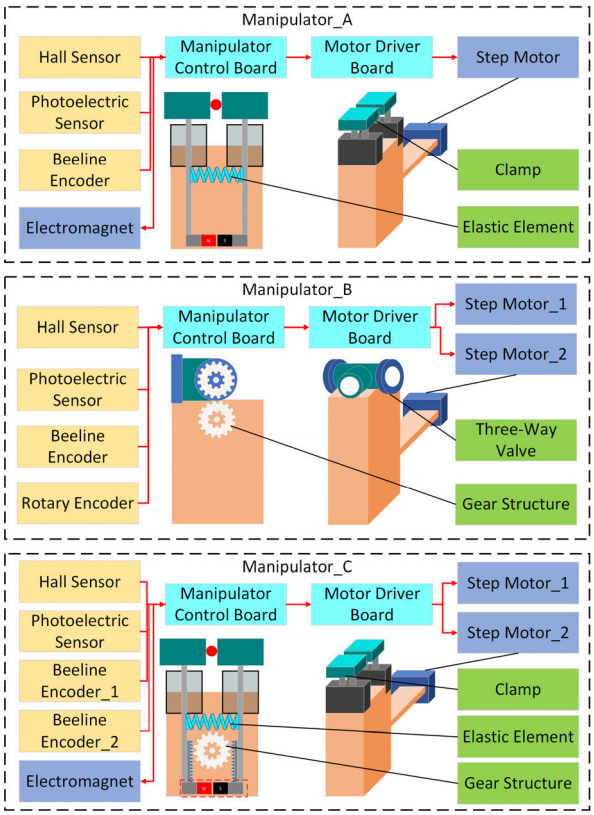

Fig. 3. Functional structure diagram of manipulators.

electromagnet is energized, it generates a force of attraction that can clamp the catheter. By default, when the electromagnet is powered OFF, the clamp is kept in a loose state through the elastic element, which is the initial state of manipulator A. When the catheter needs to be delivered, manipulator A will carry out reciprocating delivery in its interval limit. At this time, manipulators B and C will cooperate with manipulator A.

Authorized licensed use limited to: Shenzhen Technology University. Downloaded on January 02,2024 at 13:21:42 UTC from IEEE Xplore. Restrictions apply.

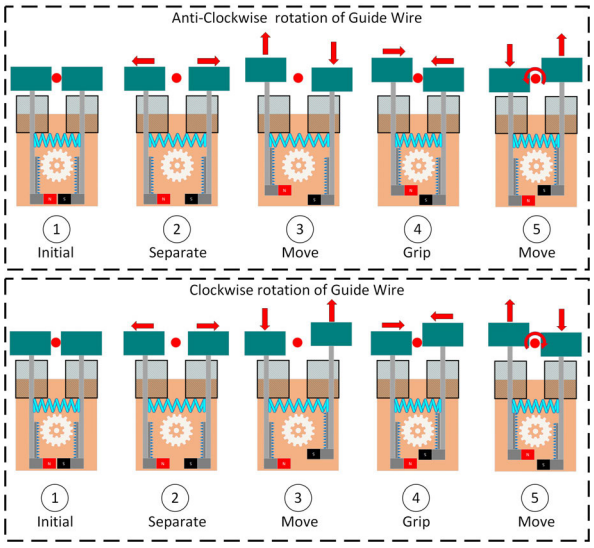

Fig. 4. Twisting steps of the guidewire.

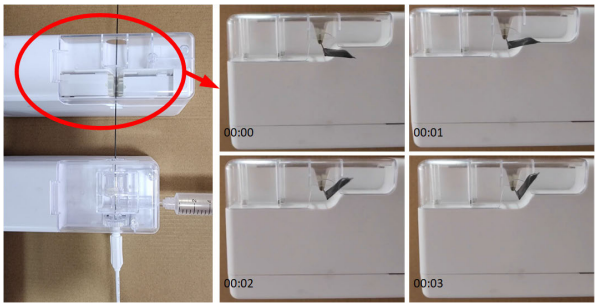

Fig. 5. Manipulator C and sterile box.

When the catheter needs to be rotated, manipulator B will drive its stepper motor_1 to rotate the end of the catheter through the gear set and read the rotation angle using the rotary encoder.

The guidewire's delivery and rotation function are entirely realized by manipulator C in Fig. 4. Stepper motor_1 realizes the rotation function, drives the fixture to rise and fall through the gear set, reads the rising and falling displacement through the linear encoder, and controls the rotation angle of the guidewire. Fig. 5 shows the process of manipulator C to realize the twisting of the guidewire. First, the clamp is opened, and then, it is lifted to the limit position. After clamping the guidewire, the torque is generated through the clamping plane's relative movement to realize the guidewire's clockwise and counterclockwise rotation.

B. Master Controller Design

Figs. 6 and 7 show the schematic of the master controller. The upper part is the initialization position of the master controller. Currently, the handle is just in the middle of the stroke. The installed photoelectric sensor determines whether the slider is initialized in place.

In terms of the operating method, our designed robot retains the doctor's operating method and muscle memory, allowing for a seamless transition without the need for changes in techniques. This design restores the catheter and guidewire manipulation techniques used in manual surgery. In the control system, we have adopted a master–slave follow mechanism. This method replicates the real-life experience of doctors during operations. The instrument follows the doctor's movements in real time, where the distance and speed are directly determined by the doctor, rather than controlling the instrument's distance through the duration of a timed action. As a result, compared to other interventional robot operating systems, such as CorPath GRX, Sensei X2, or other control methods, our design significantly reduces the learning cost for doctors. Doctors can immediately perform the surgery without the need for additional learning of the operating method.

The following part is the status after the right side of the master controller handle is moved. The controller is divided into symmetrical left and right sides. The left side represents the catheter movement, and the right side represents the guidewire movement, which is consistent with the operation mode and direction of the doctor in the actual operation.

The handle, inductive metal ring, rack, and slider are components that can move in a straight line along the slide rail. At the same time, the handle can also rotate in addition to moving in a straight line. The grating encoder collects the rotation angle, and the beeline encoder collects the moving displacement to the embedded control system. There are two main functions of the metal rod: one is used as a guide rail to support the sliding of the handle, and the other is to transmit signals, connect the inductive metal ring to the embedded board through the metal rod, and collect the signal through the contact sensing chip to judge whether the doctor holds the handle without additional doctor's operation. When the handle moves to other positions during operation, releasing the handle will automatically reset to the initial position under the drive of the stepping motor and the gear set. The gear connection part of the stepping motor and the handle will trigger the clutch during operation so that the connection between the gear set and the rotating shaft of the stepping motor is decoupled, reducing the handle's resistance in operation.

The movement distance of the master controller handle corresponds to the catheter and guidewire. When the doctor holds the handle, the slave manipulator will clamp the corresponding catheter or guidewire. For example, the right handle corresponds to the guidewire. When the handle holds and moves h distance to the right, the guidewire at the slave robot will move h distance accordingly and keep synchronized with the movement of the master handle.

C. Collaboration Strategy

The operation mode of the master controller to the slave robot and the cooperation strategy between the slave robot are shown in Fig. 6. This figure takes the catheter side as an example to show the operation steps of the catheter. Because the structure of the master controller of the guidewire and catheter is symmetrical, the difference is not significant. First, in the first step, the doctor holds the left handle of the master controller with his left hand, and manipulator A holds it. Currently, the catheter and manipulator A form a whole. In Step 2, the doctor holds the handle and moves it to the left for d distance, which means that the catheter needs to

Authorized licensed use limited to: Shenzhen Technology University. Downloaded on January 02,2024 at 13:21:42 UTC from IEEE Xplore. Restrictions apply.

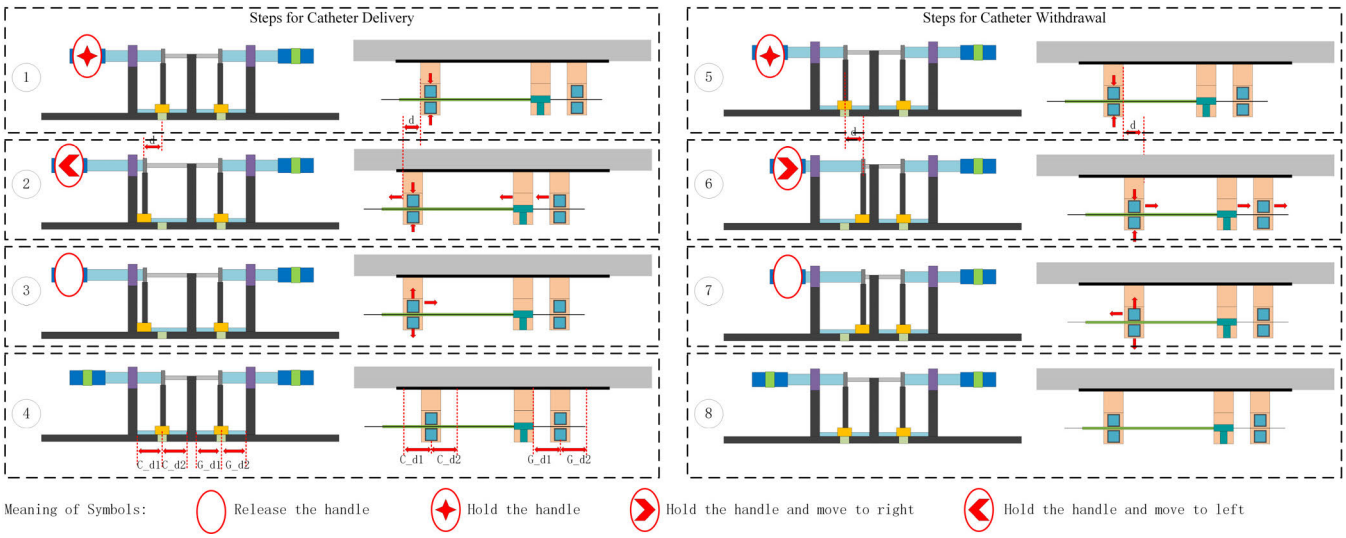

Fig. 6. Master–slave collaborative control strategy.

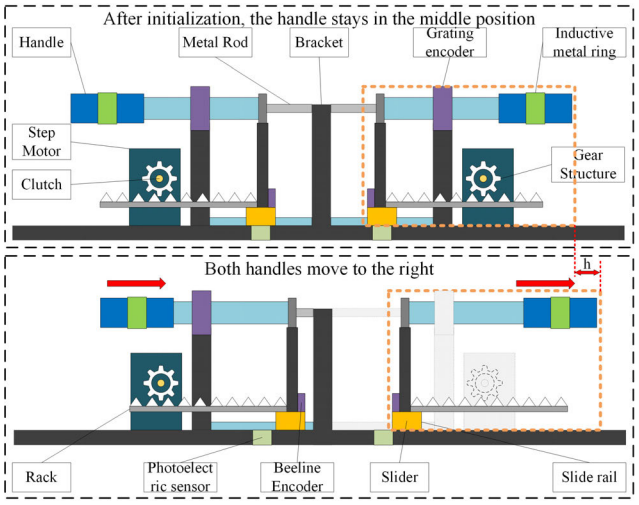

Fig. 7. Structure diagram of the master controller.

deliver d distance forward. At this time, manipulator A will clamp the catheter for d distance, and manipulators B and C will follow manipulator A for d distance. Here, it needs to be explained in advance that the range of motion of manipulators A and C along the axis of the catheter is the same as that of the master controller handles. Hence, there is a mechanical limit for the maximum distance of each delivery by the doctor. In Step 3, when the catheter handle is released, the slave manipulator A will return to the initial position shown in step 4, and the master controller handle will also reset, waiting for the next operation. The catheter withdrawal procedure is like the delivery procedure. While manipulator A moves with the handle, manipulators B and C will move with manipulator A. Still, manipulator A must be reset after each operation, and manipulators B and C do not need to reset. When manipulators B and C reach the limit, they will stop moving. The control strategy of the guidewire is the same as that of the catheter. Still, the delivery and withdrawal distance of the guidewire is determined by the relative movement distance of B and C.

The specific control process of the manipulator is shown in Fig. 6. When the doctor holds the handle, it will be mapped to the catheter and guidewire according to the motion state of the handle. In the design of the robot system, the axial translation and rotation are completely decoupled, and the two actions can be realized simultaneously. According to the actual operation situation, the catheter and guidewire move together in algorithm design, which is from the doctor's operation habit. Because the catheter and the guidewire are required to cooperate during the operation, the catheter and the guidewire are both moving forward at the same time except for the sheath placement process, and the motion of the guidewire is mainly relative to the end of the catheter, which plays a guiding role. Therefore, the advance and retreat of the guidewire are based on the catheter, that is, the forward and backward of manipulator C are determined relative to manipulator B.

D. Control and Driving System

The hardware connection relationship of the endovascular intervention robot is shown in Fig. 8, which is divided into three components: the master controller, the slave actuator, and the gantry. The whole power supply of the robot is introduced from the gantry. After ac-to-dc and filtering, 24-V dc voltage is obtained and supplied to the slave actuator and master controller. In addition, the gantry is also equipped with two stepper motors, namely, Gantry Motor_1 and Gantry Motor_2. Realize the surgical position adjustment of the slave actuator with two degrees of freedom. In the control architecture design of the system, we adopted a modular design scheme. Each manipulator becomes a separate system, comprising a manipulator control board, manipulator drive board, actuator, and encoder. The manipulator control board is mainly responsible for connecting various sensors and electromagnets, communicating with the slave control board and manipulator drive board, and receiving and sending control information. Each manipulator control board has its number, and the program will determine the position and control strategy of the manipulator according to the number to facilitate mass production.

Authorized licensed use limited to: Shenzhen Technology University. Downloaded on January 02,2024 at 13:21:42 UTC from IEEE Xplore. Restrictions apply.

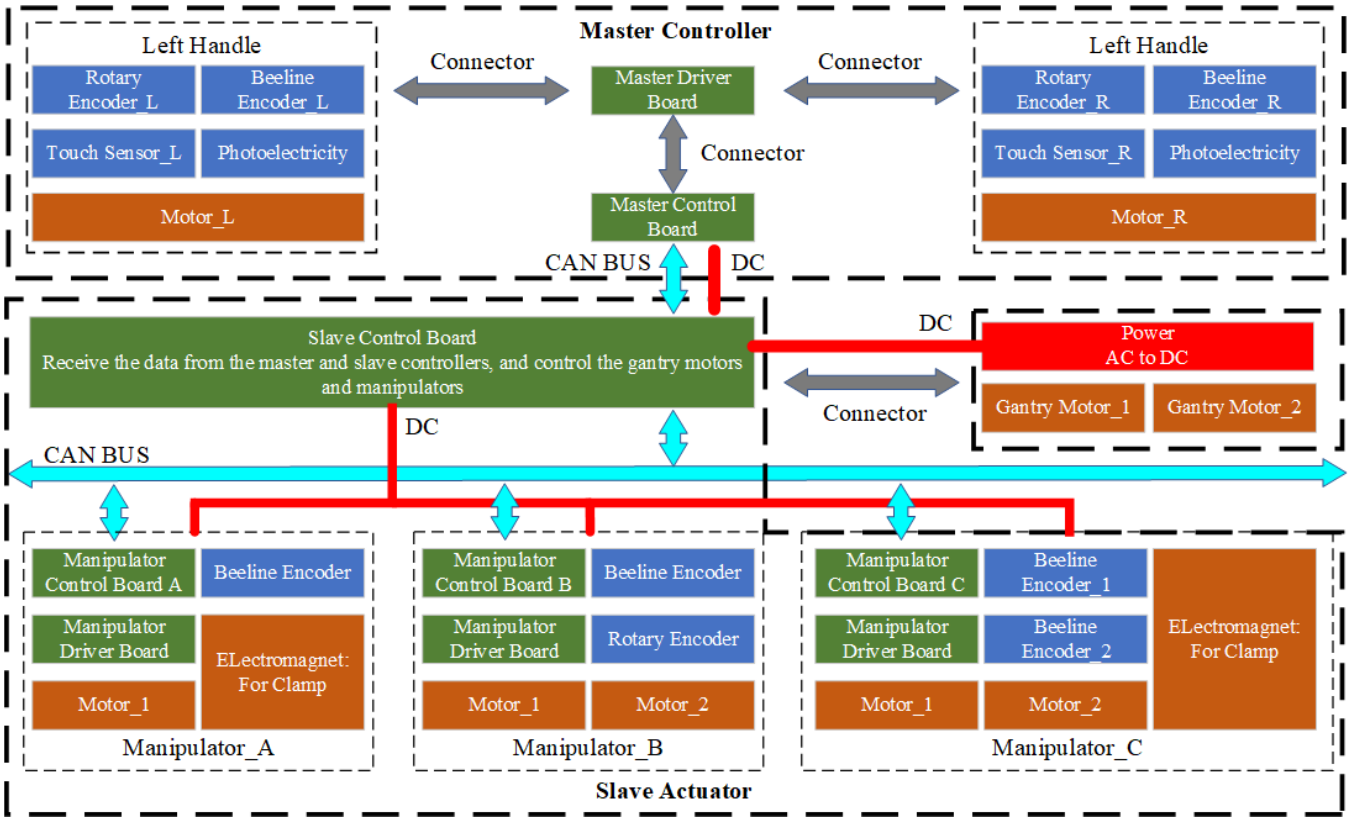

Fig. 8. Architecture of the endovascular intervention robot control system.

The driving board of the manipulator adopts a motor driving chip, which is mainly responsible for driving and controlling the stepping motor. Manipulator A has only one stepper motor to realize the overall movement of the manipulator along the slave actuator guide rail. The clamping is completed by the electromagnet, with two degrees of freedom. In addition to the stepper motor that moves along the guide rail at the slave end, manipulator B also has a stepper motor that realizes the rotation of the end of the catheter.

However, because the clamping function is not required, there is no electromagnet, with a total of two degrees of freedom. Manipulator C needs two stepper motors and one electromagnet for clamping, rotating, and delivering the guidewire simultaneously, with three degrees of freedom. The slave control board uses an STM32 chip as an MCU. Its primary function is to receive the data sent by the master controller and the slave controller, cooperate with the touch screen of the slave controller, realize the robot initialization, adjust the surgical position, replace the instrument, and monitor the robot's motion status.

The master controller contains two sets of symmetrical handles, which are connected to the master drive board at the same time. The board contains an STM32 chip responsible for connecting the sensor, running the program, and communicating with the master control board.

Then, the master control board packages the data and forwards it to the controller area network (CAN) bus. The specific connection relationship of the main line is shown in Fig. 9. The master control board is also responsible for the

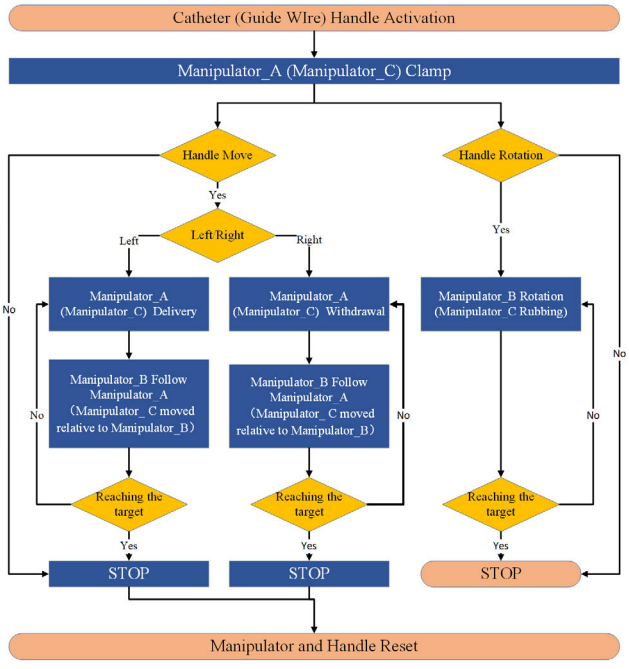

Fig. 9. Flowchart of manipulator control algorithm.

touch screen display interaction of the master controller to realize the touch operation. To keep the doctor's operating habits, our robot's master controller is designed to interact with the doctor using the two-handed handle to simulate the guidewire and the catheter. This interaction mode is different from the ordinary because the rocker and key do not need to

Authorized licensed use limited to: Shenzhen Technology University. Downloaded on January 02,2024 at 13:21:42 UTC from IEEE Xplore. Restrictions apply.

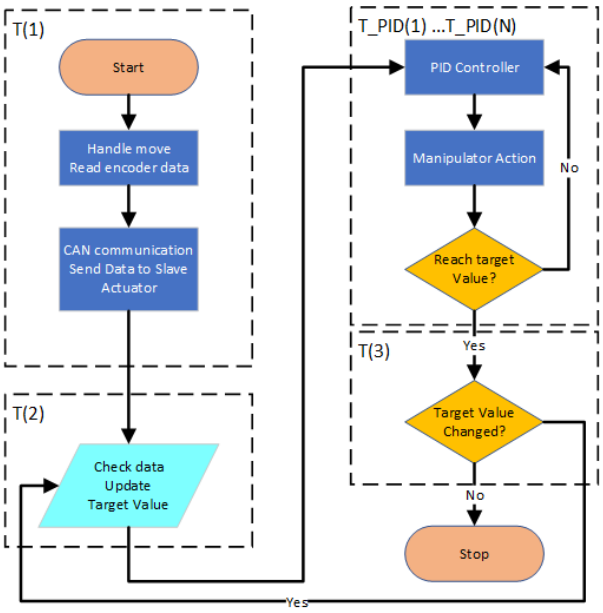

Fig. 10. Flowchart of manipulator following algorithm.

sense the speed of the doctor's hand, which is a time-triggered method. The movement of the slave manipulator can be fixed into a multilevel rate set by the master controller. However, the operation mode we designed requires the slave manipulator to follow the master handle to move synchronously in position and speed. Therefore, the performance of the stepping motor needs to be adapted according to the maximum operating speed of the doctor. Here, there are two main factors affecting the following performance. The first is the communication delay. This is the information transmission process from the master to the slave robot. The second is the time it takes for the stepper motor to reach the target position. This includes the program calculation process, mechanical structure transmission, and motor operation.

Therefore, to solve this problem, we have designed the following algorithm, as shown in Fig. 10. This algorithm is based on the traditional proportional–integral–differential (PID) controller and realizes data feedback through the encoder and data transmission through the CAN bus. First, at T(1) moment, the master handle moves an amount of displacement under the doctor's control, and the displacement direction and distance data are sent to the slave control board through the master control board on the CAN bus. At T(2) moment, after receiving the drive command from the slave control board, the manipulator corresponding to the master handle will constantly adjust the PID control algorithm to drive the stepping motor and enter the PID control process.

According to the control cycle T_PID tracking target, the PID control process will not stop immediately when the target at time T(1) has been completed. Instead, at time T(3), further, judge whether the handle displacement has changed in the control cycle. If it has changed, synchronously update the accumulated data to the new target and then continue tracking until the target has not changed within a communication interval. At this time, the following algorithm will end. This design considers the stepping motor's start, stop, and jitter,

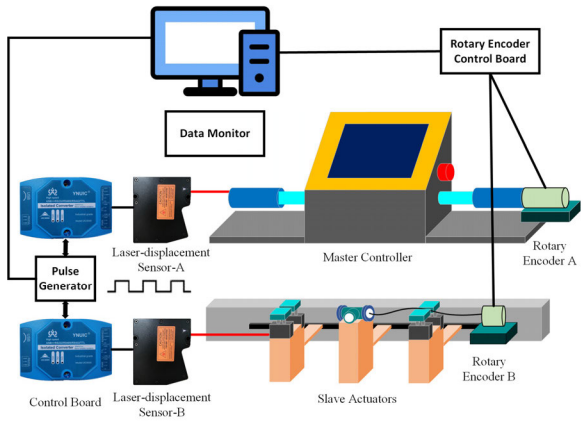

Fig. 11. Experimental environment for kinematics performance measurement.

which can effectively improve the following performance and reduce the motor noise.

IV. Experiments

This research experiment consists of two parts. The first part involves a type inspection conducted at the Shenzhen Testing Center of Medical Devices, which evaluates the overall performance in accordance with GB9706.1-2020 (Medical electrical equipment—Part 1: General requirements for basic safety and essential performance) and GB/T 14710-2009 (Environmental requirement and test methods for medical electrical equipment). The robot has passed the environmental test, collision test, and transportation test according to the abovementioned testing criteria, ensuring the safety and stability of the system.

The in vivo experiment shows the actual operation effect of the robot in endovascular interventional surgery, including the operation duration, the angiography duration, the single angiography duration, the bedside radiation dose, and the radiation dose received by the surgeon.

The coronary artery system of domestic pigs is in a similar fashion to human coronary arteries. Cardiac catheterization techniques in the pigs are similar to the techniques used in humans. Standard human diagnostic and interventional equipment can also be used. Thus, coronary arteries in domestic swine are suitable for the assessment of catheter-based interventional devices that may be used in humans [19]. In general, it is thought that the young human heart may be somewhat "pig-like," whereas the older heart with ischemic heart disease (which promotes collateral growth) may be more "dog-like" [20].

In vivo experimental setup and surgical procedures are consistent with the requirements of human clinical experiments. The experimental environment is equipped with medical devices, such as surgical beds and DSA imaging systems for angiography procedures. The surgical process includes preoperative preparation, angiography surgery, and postoperative disassembly stages. At the end of the experiment, a postoperative pathological section examination was performed on the target blood vessels.

The experimental platform for performance testing is shown in Fig. 11. We have used two sets of laser triangular displacement sensors, TS-P150, to detect the displacement of the

Authorized licensed use limited to: Shenzhen Technology University. Downloaded on January 02,2024 at 13:21:42 UTC from IEEE Xplore. Restrictions apply.

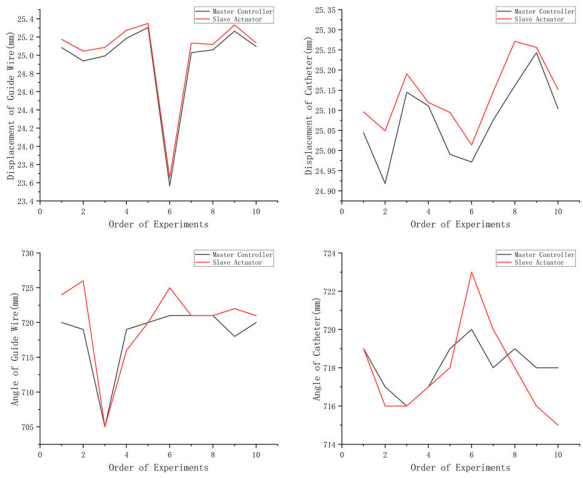

Fig. 12. Rotation and delivery data in different experimental order.

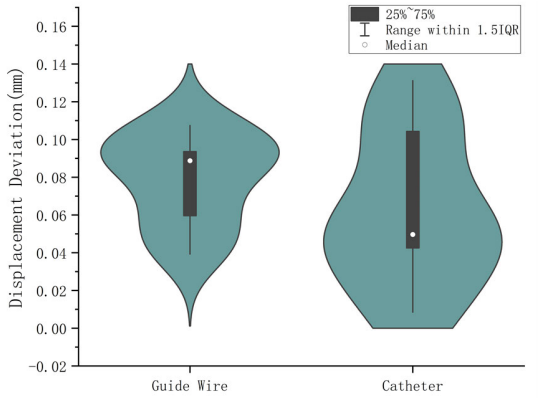

Fig. 13. Displacement error of catheter and guidewire.

push–pull rod of the master controller and the displacement of the manipulator. The sensors are connected to a pulse signal generator to ensure real-time measurement results. In addition, two sets of rotary encoders were used to measure the rotation angle of the rod and the catheter and guidewire fixed to the manipulator. Then, the data monitor can directly record and count displacement and angle data. Using this experimental platform, we tested the data shown in Figs. 12–14, including positional accuracy, rotational accuracy, and repeatability.

A. Kinematics Performance Measurement

The manipulator has a rotation resolution of 0.07° for catheter and 0.22° for guidewire. All manipulators have a linear displacement resolution of 4 μm. As shown in Fig. 13, the main controller pushes 25 mm, and the catheter average error is 0.0625 mm (0.25%), while the guidewire average error is 0.0788 mm (0.32%). Therefore, the synchronous accuracy error between the catheter and guidewire is 0.0163 mm (0.0652%). However, as shown in Fig. 14, in the rotation function, the twisting method of the guidewire is not as accurate as the gear rotation method of the catheter.

As shown in Tables I–III, this robot supports catheters with specifications of 4F, 5F, and 6F, with a length range of 100–130 cm, and 0.035-in guidewire, with a length range

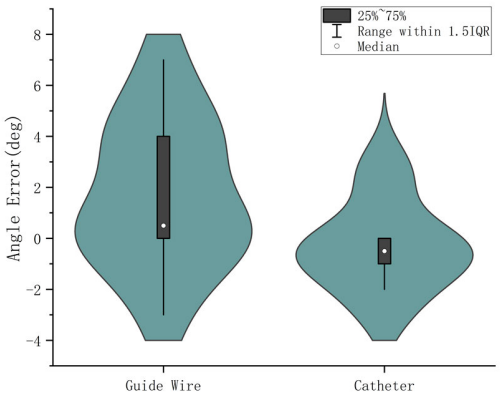

Fig. 14. Angle error of catheter and guidewire.

TABLE I
SUPPORTED INTERVENTIONAL DEVICES

Instruments	Spec	Length(±5%)
Catheter	4F/5F/6F	100cm-130cm
Guidewire	0.035inch	150cm-180cm

TABLE II
MOTION PERFORMANCE BASED ON TYPE INSPECTION

Instruments	Maximum Operating Speed	Master-slave Follow Delay
Catheter	110.68mm/s	37ms
Guidewire	119.55mm/s	35ms

TABLE III
ACCURACY BASED ON TYPE INSPECTION

Instruments	Linear Accuracy	Linear Repeatability	Rotation Accuracy
Catheter	0.0625mm	0.0389mm	-0.3°
Guidewire	0.0788mm	0.023mm	+1.7°

of 150–180 cm, which covers most of the interventional instruments for angiographic surgery. The total delay from the initial operation to the final response is 37 ms for the catheter and 35 ms for the guidewire. The acceptable time delay of a visual–haptic interface strongly depends on the application and can be as small as 45 ms [21]. According to the feedback from medical professionals and relevant literature, this delay can meet the requirements for remote surgery.

The linear distance accuracy requirement is less than 0.1 mm, the repeatability requirement is less than 0.05 mm, and the rotation accuracy requirement is less than 10°. These technical indicators are derived from research on the actual surgical needs of vascular interventional physicians. The maximum forward speed of the catheter is 110.68 mm/s, the master and slave follow delay can be extended for 37 ms, the linear motion distance error is 0.0625 mm, the repeatability is 0.041 mm, and the rotation accuracy is −0.3°. The maximum forward speed of the guidewire is 119.55 mm/s, the master and slave follow delay is 35 ms, and the linear motion distance error is 0.0788 mm; the repeatability is 0.0242 mm and the rotation accuracy is +1.7°.

Authorized licensed use limited to: Shenzhen Technology University. Downloaded on January 02,2024 at 13:21:42 UTC from IEEE Xplore. Restrictions apply.

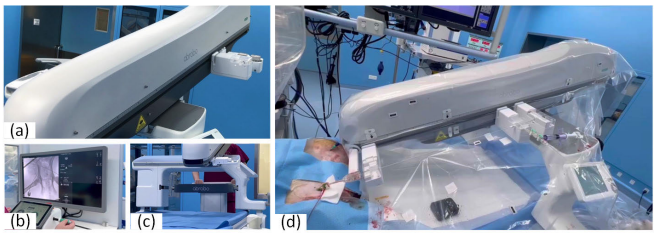

Fig. 15. In vivo experiment and endovascular intervention robot. (a) Slave Robot. (b) Master controller. (c) Gantry. (d) Experimental environment.

TABLE IV
ACCURACY BASED ON TYPE INSPECTION

Order	Operations	Animal Breed	Number of Vessels
1	Cerebral	Bama Pig	4
2	Cerebral	Bama Pig	4
3	Cerebral	Bama Pig	4
4	Cerebral	Bama Pig	8
5	Cerebral	Bama Pig	3
6	Coronary	Bama Pig	3
7	Cerebral	Bama Pig	3
8	Cerebral	Bama Pig	6
9	Cerebral	Golden Retriever	7
10	Cerebral	Bama Pig	8
11	Coronary	Bama Pig	2
12	Cerebral	Bama Pig	7

The distal end of the catheters (4F, 5F, and 6F) are securely fixed to the three-way valve and rotated through a gear drive. Therefore, the performance experiments use a laser rangefinder to directly detect the displacement deviation of the manipulator. Subsequently, the catheters are clamped in the rotating test fixture, and the rotation angle is measured using an encoder. The guidewire is not fixed by a controller but is instead compressed using the planar gripping method of manipulator C and rotated through twisting. All supported interventional instruments in Table I can be stably fixed and move smoothly during the process without bending or twisting.

B. In Vivo Experiments

The immediate environment of the in vivo experiment is shown in Fig. 15, in which Fig. 15(a) shows the main body of the slave robot, including the gantry and the slave actuator, and Fig. 15(b) shows the radiation protection console and the master controller, where doctors perform remote operations, and the console screen can display DSA images. Fig. 15(c) shows how the medical staff installs the robot on the operating table by operating the auxiliary trolley. Fig. 15(d) shows the sterile cover, sterile box, and slave robot during the in vivo experiment.

As can be seen from Table IV, we conducted 12 in vivo experiments, including 11 Bama pigs, one golden retriever dog, ten cerebral angiography operations, and two coronary angiography operations, all of which successfully assisted doctors in achieving control of the guidewire and catheter, complete vascular superselective, and angiography,

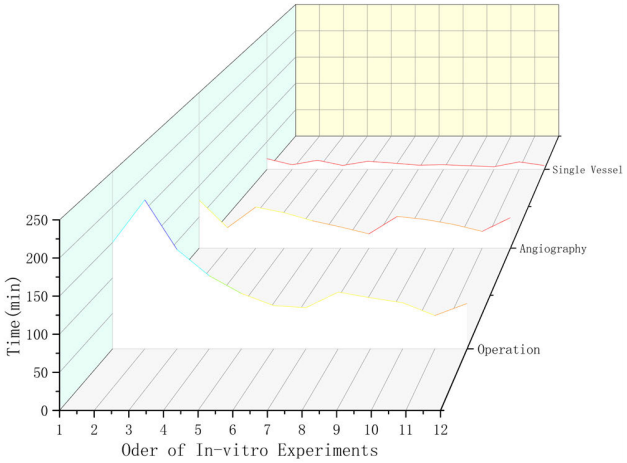

Fig. 16. Time of operation, angiography, and single vessel angiography in a different order.

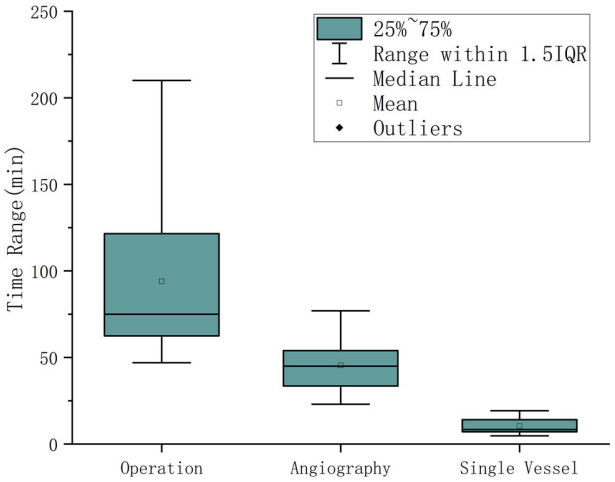

Fig. 17. Average operation time, angiography, and single vessel angiography.

and observed that no apparent damage was caused to the vascular wall through postoperative pathological sections, meeting the surgical expectations.

In Figs. 16 and 17, we can see the operation time, angiography time, and single vascular angiography time and their statistical data corresponding to different sequence experiments. The average operation time is 94.00 min, the average angiography time is 45.42 min, and the average single root angiography time is 10.43 min.

As shown in Fig. 18, the radiation amount near the operating bed and the radiation dose of the doctor are recorded, respectively, in which the average radiation amount at the bedside is 114.58 μSv and the average radiation dose of the doctor is 1.38 μSv; compared with traditional surgery, this reduces the radiation injury by 98.68% and effectively protects the health of doctors. In Fig. 19, the data analysis of typical vascular pathological sections from Wuhan Servicebio Technology Company provides evidence of the safety of the surgery.

The comparative analysis of linear accuracy was conducted in Table V between the research studies of Wang et al.

Authorized licensed use limited to: Shenzhen Technology University. Downloaded on January 02,2024 at 13:21:42 UTC from IEEE Xplore. Restrictions apply.

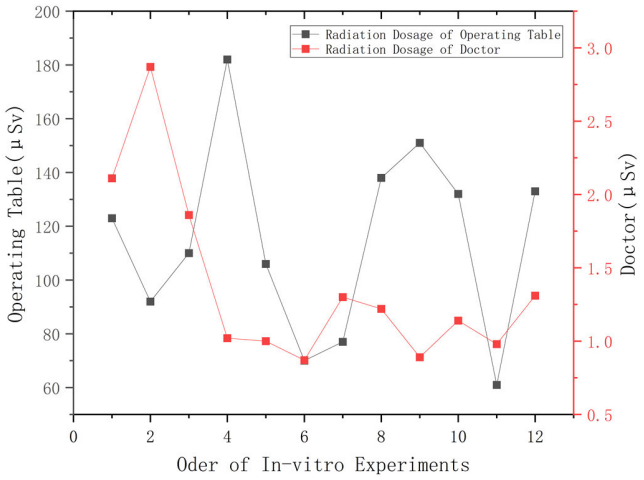

Fig. 18. Radiation dosage of operating table and doctor in different order.

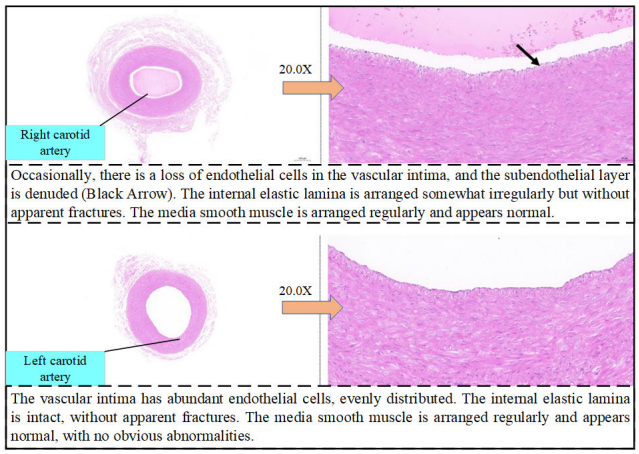

Fig. 19. Analysis of typical pathological section data of left coronary artery and right coronary artery.

TABLE V
COMPARATIVE ANALYSIS OF LINEAR ACCURACY

Intervention Robots	Linear Accuracy
Our robot	Average Less than 0.1mm
Wang. K et al.	0.5 mm
Omisore et al.	0.4 mm
H. Wang et al.	0.07 mm-0.3 mm

(0.5 mm), Omisore et al. (0.4 mm), and Wang et al. (0.07–0.3 mm). The endovascular intervention robot in this study exhibits superior precision of linear accuracy (average less than 0.1 mm) [3].

V. CONCLUSION

A reciprocating delivery device-based endovascular intervention robot with multimanipulators collaboration is proposed. The cooperative control strategy of the multimanipulator, the control system architecture, and the closed-loop control algorithm are designed. To verify the feasibility, safety, and efficacy of the interventional robot, type inspection and 12 in vivo experiments were carried out. The experimental results showed that the robot is compatible with the commonly used 4F–6F imaging catheter and 0.035-in guidewire. The following delay and control accuracy meet the surgical requirements. The master controller preserved the clinical experience for doctors, and the average single root angiography time is only 10.43 min. Compared with traditional interventional surgery, the whole system reduces the radiation dose for doctors by nearly 98.68%. This study demonstrated the feasibility, safety, and efficacy of the system. The endovascular intervention robot met the expected technical and simulated clinical performance.

REFERENCES

[1] D. Adam et al., "World population hits eight billion—Here's how researchers predict it will grow," *Nature*, Nov. 2022. [Online]. Available: https://www.nature.com/articles/d41586-022-03720-6
[2] C. W. Tsao et al., "Heart disease and stroke statistics-2022 update: A report from the American Heart Association," *Circulation*, vol. 145, no. 8, pp. 153–639, 2022.
[3] W. Duan et al., "Technical and clinical progress on robot-assisted endovascular interventions: A review," *Micromachines*, vol. 14, no. 1, p. 197, Jan. 2023.
[4] F. Giurazza et al., "Post-traumatic intraparenchymal renal hemorrhages: Correlation between CT and DSA vascular findings for superselective embolization procedures," *Diagnostics*, vol. 11, no. 7, p. 1256, Jul. 2021.
[5] X. Jin, S. Guo, J. Guo, P. Shi, M. Kawanishi, and H. Hirata, "Active suppression method of dangerous behaviors for robot-assisted vascular interventional surgery," *IEEE Trans. Instrum. Meas.*, vol. 71, pp. 1–9, 2022.
[6] C. Yang, S. Guo, Y. Guo, and X. Bao, "Cloud communication-based sensing performance evaluation of a vascular interventional robot system," *IEEE Sensors J.*, vol. 22, no. 9, pp. 9005–9017, May 2022.
[7] W. Zhou, S. Guo, J. Guo, F. Meng, Z. Chen, and C. Lyu, "A surgeon's habits-based novel master manipulator for the vascular interventional surgical master-slave robotic system," *IEEE Sensors J.*, vol. 22, no. 10, pp. 9922–9931, May 2022.
[8] X. Jin et al., "Total force analysis and safety enhancing for operating both guidewire and catheter in endovascular surgery," *IEEE Sensors J.*, vol. 21, no. 20, pp. 22499–22509, Oct. 2021.
[9] C. Lyu et al., "A deep-learning-based guidewire compliant control method for the endovascular surgery robot," *Micromachines*, vol. 13, no. 12, p. 2237, Dec. 2022.
[10] Y. Yan, S. Guo, C. Lyu, D. Zhao, and Z. Lin, "SEA-based humanoid finger-functional parallel gripper with two actuators: PG2 gripper," *IEEE Trans. Instrum. Meas.*, vol. 72, pp. 1–13, 2023.
[11] Y. Zhao et al., "Surgical GAN: Towards real-time path planning for passive flexible tools in endovascular surgeries," *Neurocomputing*, vol. 500, pp. 567–580, Aug. 2022.
[12] X. Bao et al., "Multilevel operation strategy of a vascular interventional robot system for surgical safety in teleoperation," *IEEE Trans. Robot.*, vol. 38, no. 4, pp. 2238–2250, Aug. 2022.
[13] Y. Wang, J. Wang, Y. Li, T. Yang, and C. Ren, "The deep reinforcement learning-based VR training system with haptic guidance for catheterization skill transfer," *IEEE Sensors J.*, vol. 22, no. 23, pp. 23356–23366, Dec. 2022.
[14] G. Najafi, K. Kreiser, M. E. M. K. Abdelaziz, and M. S. Hamady, "Current state of robotics in interventional radiology," *CardioVascular Interventional Radiol.*, vol. 46, no. 5, pp. 549–561, May 2023.
[15] A. Stevenson, A. Kirresh, M. Ahmad, and L. Candilio, "Robotic-assisted PCI: The future of coronary intervention?" *Cardiovascular Revascularization Med.*, vol. 35, pp. 161–168, Feb. 2022.
[16] R. Beyar, J. E. Davies, C. Cook, D. Dudek, P. A. Cummins, and N. Bruining, "Robotics, imaging, and artificial intelligence in the catheterisation laboratory," *EuroIntervention*, vol. 17, no. 7, pp. 537–549, Sep. 2021.
[17] H.-S. Song, J.-H. Woo, J.-Y. Won, and B.-J. Yi, "In vivo usability test of vascular intervention robotic system controlled by two types of master devices," *Appl. Sci.*, vol. 11, no. 12, p. 5453, Jun. 2021.
[18] Y. Kim et al., "Telerobotic neurovascular interventions with magnetic manipulation," *Sci. Robot.*, vol. 7, no. 65, p. 9907, Apr. 2022.

Authorized licensed use limited to: Shenzhen Technology University. Downloaded on January 02,2024 at 13:21:42 UTC from IEEE Xplore. Restrictions apply.

[19] Y. Suzuki, A. C. Yeung, and F. Ikeno, "The representative porcine model for human cardiovascular disease," *BioMed Res. Int.*, vol. 2011, pp. 1–10, Jan. 2011.
[20] P. Camacho, H. Fan, Z. Liu, and J.-Q. He, "Large mammalian animal models of heart disease," *J. Cardiovascular Develop. Disease*, vol. 3, no. 4, p. 30, Oct. 2016.
[21] I. M. L. C. Vogels, "Detection of temporal delays in visual-haptic interfaces," *Human Factors, J. Human Factors Ergonom. Soc.*, vol. 46, no. 1, pp. 118–134, Mar. 2004.

Sheng Cao (Graduate Student Member, IEEE) received the B.S. degree in power system and automation from the Army Engineering University of PLA, Nanjing, China, in 2018, and the M.S. degree in control science and engineering from the Tianjin University of Technology, Tianjin, China, in 2021. He is currently pursuing the Ph.D. degree with the School of Life Science, Beijing Institute of Technology, Beijing, China.

Shuxiang Guo (Fellow, IEEE) is currently a Chair Professor with the Southern University of Science and Technology, Shenzhen, China. He is also a Chair Professor with the Beijing Institute of Technology, Beijing, China.

Prof. Guo has a fellowship of the Engineering Academy of Japan.

Jian Guo is currently a part-time Professor with the School of Electrical Engineering and Automation, Tianjin University of Technology, Tianjin, China. He is also the CEO of Shenzhen Institute of Advanced Biomedical Robot Company Ltd., Shenzhen, China.

Jian Wang received the B.Sc. degree from the Changchun Institute of Optics and Fine Mechanics, Changchun, China, in 2001, and the M.Sc. and Ph.D. degrees from Kagawa University, Takamatsu, Japan, in 2005 and 2008, respectively.

He is currently the Chief Engineer with the Shenzhen Institute of Advanced Biomedical Robot Company Ltd., in Shenzhen, China.

Yongxin Zhang received the Doctor of Philosophy and medical doctor's degree from the Second Military Medical University, China, in 2017.

He is currently the Secretary of the OCIN imaging core-lab, China. His representative papers have been published in NEJM and the Lancet.

Yongwei Zhang is skilled in the field of neurointerventional treatment with 20 years of experience and was one of the early surgeons in the interventional treatment of acute ischemia stroke in China. He is currently the Vice Director of the Neurovascular Center, Shanghai Changhai Hospital, Naval Medical University, Shanghai, China.

Pengfei Yang is currently the Executive Director of the Neurovascular Center, Shanghai Changhai Hospital, Naval Medical University, Shanghai, China, and the Vice Director of the Institute of Cerebrovascular Diseases of the PLA, Shanghai.

Jianmin Liu is currently the Director of the Neurovascular Center, Shanghai Changhai Hospital, Shanghai, China, and the Director of the Institute of Cerebrovascular Disease of the PLA, Shanghai.

Authorized licensed use limited to: Shenzhen Technology University. Downloaded on January 02,2024 at 13:21:42 UTC from IEEE Xplore. Restrictions apply.